Sensors & Transducers, Vol. 160, Issue 12, December 2013, pp. 63-67

Sensors & Transducers

Inclination Measurement Based on MEMS Accelerometer

Zhengqin LI
Information Engineering Branch, City College, Wenzhou University, 325035, China
[1] Tel.: 0086-577-86698888, 0086-fax: 0577-86698888
E-mail: zhengqin_li@yeah.net

Received: 23 September 2013 /Accepted: 22 November 2013 /Published: 30 December 2013

Abstract: MEMS accelerometer is very suitable for dip angle measurement with its small size, low power consumption and so on. The working principle of MEMS accelerometer was described in this study, and using the accelerometer to measure inclination was analyzed. Triaxial digital chip ADXL345 of acceleration was controlled via SPI mode driving using MSP430F149 microcontroller, and interface circuit and driver were designed, thus successfully achieving inclination measurement. Moreover, error is ±0.3°, and resolution may be up to 0.015°, while measuring system has the advantage of low power consumption. *Copyright © 2013 IFSA.*

Keywords: Accelerometer; MEMS, Inclination measurement.

1. Introduction

Inclination needs to be measured in many engineering applications at present. Whether some plane is in a horizontal, vertical position or its angle relative to horizontal surface is measured. Then, these measured values are used to monitor or control the system. MEMS (Micro Electro Mechanical System) accelerometer is small in size, low in power consumption and cost, high in reliability and easy to implement digitalization and intelligence. The micro-mechanical structure is accurate in producing, reproducible, easy in integration, suitable for mass production and high in performance-price ratio. Therefore, use of MEMS accelerometer to measure inclination has a significant advantage. Dynamic acceleration caused by motion or shock by the triaxial MEMS accelerometer ADXL345 of MSP430F149 microcontroller driving can be measured in this study. Static acceleration such as gravity acceleration can also be measured by it. Inclination measurement and display can be easily achieved by extending the display device.

2. Work Principle of MEMS Accelerometer

MEMS accelerometer often uses the micromachined structure of polysilicon surface and is placed at the top of wafer. Polysilicon spring is hung over the surface structure of wafer in the measurement of acceleration to provide strength resistance. Differential capacitance consists of independent fixed plate and activity quality connecting plate, and structure deflection can be measured by it. Acceleration makes inertial mass deflected and differential capacitance unbalance. The capacitance value changes of two differential capacitances are converted to voltage changes by the conversion circuit. Moreover, the output voltage amplitude of sensor is directly proportional to acceleration. Acceleration polarity is determined by phase sensitive demodulation. Fig. 1 shows that active plate is driven to move when middle inertial mass does an acceleration motion. Thus, distance between active plate and fixed plate on one side is increased, and its distance away from fixed plate on the other side is correspondingly reduced. Thus, the capacitance values of differential capacitors C1 and C2 are changed, and the variation of capacitance values reflects changes in acceleration [1].

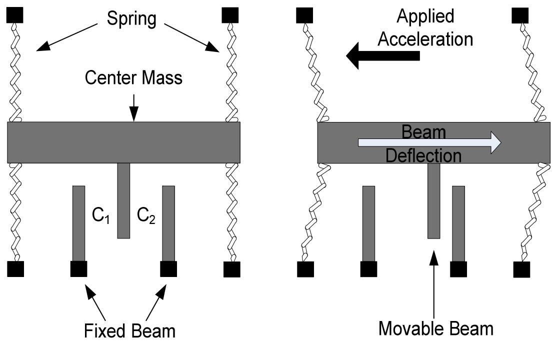

Fig. 1. Principle of operation of the MEMS acceleration sensor.

3. Theoretical Basis of Inclination Measurement

Each-axis acceleration value output by accelerometer cannot directly represent object inclination when inclination is measured, and equation conversion is needed to get dip value [2]. The initial state coordinate system of accelerometer is shown in Fig. 2 (a) when it is placed horizontally on a horizontal plane. Suppose that the angle of X axis and horizontal plane is pitch angle γ, and the angle of Y axis and horizontal plane is roll angle θ. The derivation of calculation formula was conducted with pitch angle as an example below.

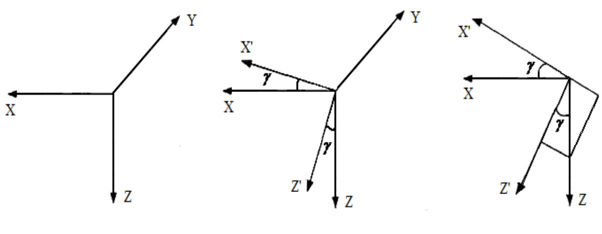

(a) (b) (c)

Fig. 2. The acceleration sensor coordinate system.

The pitch angle is 0 in initial state. If g represents the gravitational acceleration, then the static acceleration value on each axis is:

$$\begin{cases} G_x = 0g \\ G_y = 0g \\ G_z = 1g \end{cases} \tag{1}$$

The coordinate system of accelerometer is shown in Fig. 2 (b) when pitch angle γ is generated between X-axis and horizontal plane. The coordinate system is projected onto the XZ-axis plane, and thus plane coordinate system can be obtained, as shown in Fig. 2 (c). Therefore, static acceleration value can be obtained on each axis.

$$\begin{cases} G_x = -1g \times \sin\gamma \\ G_y = 0g \\ G_z = 1g \times \cos\gamma \end{cases} \tag{2}$$

The calculation formula of pitch angle can be got by the above equations:

$$\gamma = -\arctan(G_x / G_z) \tag{3}$$

The calculation formula of roll angle is similarly obtained:

$$\theta = \arctan(G_y / G_z) \tag{4}$$

Therefore, pitch angle and roll angle can be calculated by formulas (3) and (4) according to output acceleration values on the three axes of accelerometer. It should be noted that it is impossible to measure magnetic heading angle because magnetic sensor is not used to measure Earth's magnetic field [3]. Magnetic heading angle is unnecessary for general inclination measurement requirements.

4. Trixie Digital Accelerometer ADXL345

ADXL345 is a small, thin, low-power and triaxial accelerometer and can perform high resolution (13 bit) measurement on ±16 g acceleration. Digital output data is 16-bit binary complement format and can be accessed through SPI (3-wire or 4-wire) or I2C digital interface. It can measure static acceleration of gravity in skew detection applications and can also measure the dynamic acceleration caused by motion or shock. Moreover, it has a high resolution (4 mg/LSB) and is capable of measuring the inclination change of about 0.25°. Analog-digital conversion is not needed when ADXL345 and other digital output accelerometers is used. This device offers a variety of special detection functions. Active and inactive detection functions are to detect whether movement occurs by comparing the acceleration on any axis with user-set thresholds. Knock direction function is to detect single and dual vibrations in any direction. Freefall detection function is to detect whether device is falling. These functions need no host processor to perform any calculations. Built-in 32-level FIFO memory buffer can reduce the burden on the host processor and play the roles of simplification algorithm and power saving. ADXL345 is used as a "motion switch"(1) (shut down the entire system with no activity, open when activity is detected) by built-in active/inactive detection function. Therefore, the system can achieve further power saving. Figs. 3 and 4 show ADXL345 pin configuration and function block diagram, respectively [4].

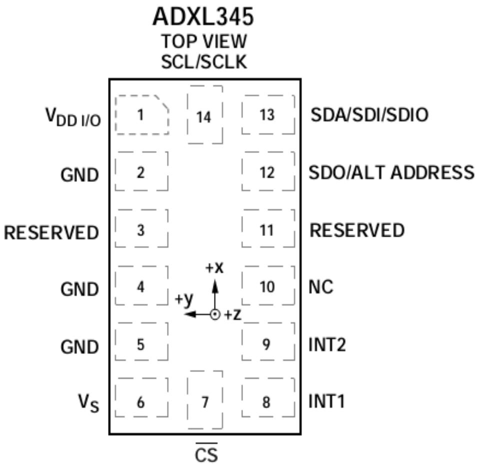

Fig. 3. Pin configuration.

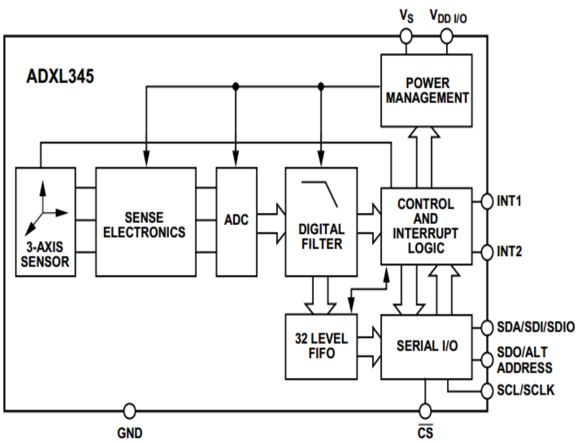

Fig. 4. Functional block diagram.

5. Typical Application of ADXL345

5.1. Interface Circuit

TI (Texas Instrument) company's microcontroller MSP430F149 driving is used to control ADXL345 to reduce power consumption. MSP430F149 microcontroller has rich peripheral modules and very low power consumption, and active mode is 200 µA with 1 MHz clock frequency and only 0.1 µA with a close mode. Moreover, it has five kinds of energy-saving work ways [5]. Combining ADXL345 automatic adjustment power, automatic sleep and standby function can effectively reduce system power consumption. ADXL345 may communicate with control chip by I2C (Inter-Integrated circuit) mode or SPI (Serial peripheral interface) mode.

Fig. 5 shows the communication with control chip by a SPI mode of four-wire system. The pin roles of ADXL345 as a slave computer in the communication process are as follows: SDI-data input, SDO-data output, INT1 and INT2-interrupt signal, SCLK-clock signal. ADXL345 $\overline{CS}$ pin is controlled by the bus host in SPI mode. MSP430F149 pins P1.1 and P1.2 are configured as an external interrupt pin by register. Both digital and analog powers of system are decoupled through 0.1 µF ceramic capacitor and 10 µF electrolytic capacitor. Digital and analog power grounds are separated and only connected at a point through 0 Ω resistor to improve the anti-jamming capability of system.

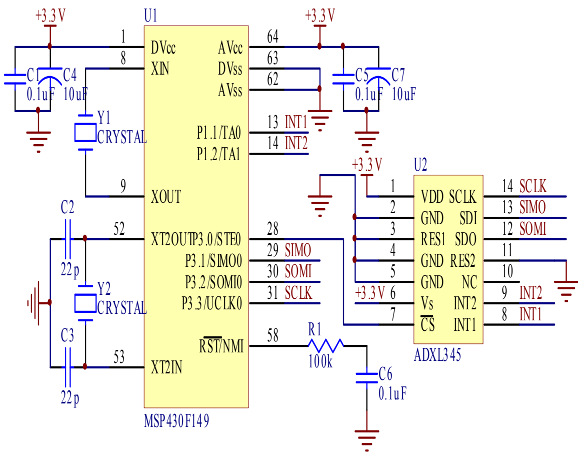

Fig. 5. Interface circuit of MSP30F149 and ADXL345.

5.2. Program Design

ADXL345 has two programmable interrupt pins: INT1 and INT2. Data_Ready and Inactivity interrupt source were first alluded to the INT1 and INT2 interrupt pins through initialization, respectively. Data_Ready interrupted set and sent the interrupt request to MSP430F149 P1.1 pin when new data was generated. MSP430F149 drew ADXL345 $\overline{CS}$ pin high in the interrupt service program, which meant that SPI transmission occurred. MSP430F149 would write instruction into ADXL345. Fig. 6 shows the 4-wire SPI timing diagram of writing. As can be seen from the figure, $\overline{CS}$ level switches at the beginning and the end of each transmission in the SPI mode. Data were updated with SCLK fall edge, and sampling was done with SCLK rising edge. The read and write operations of SPI bus to internal ADXL345 registers were performed in bytes because 30 operable registers in ADXL345 were all byte registers. A fall edge was manufactured at P3.3/SCLK pin according to the interface circuit in Fig. 5. A high bit BIT7 of data was output, and then P3.3/SCLK level was drawn high. Data in the DATA was sequentially shifted towards right by one bit, and then SCLK was drawn low. The high bit of data was output again, when the output was secondary high bit BIT6 bit in the original data. These were repeated, and the right shift of data for 8 times would complete a character output. The control of timing diagram and interface circuit achieves the multi-character subfunction code of SPI writing as follows (Fig. 6).

```
Void SpiWrite (char * Buffer, int cnt) {/ / Buffer is writing string, and cnt is string length
char data;
int i, j;
for (i = 0; i <cnt; i + +) {
data = Buffer [i];
for (j = 0; j <8; j + +) {
P3OUT & = ~ BIT3; / / SCLK fall edge is generated
if (data & BIT7) / / high bit is 1
P3OUT | = BIT1; / / P3.1 output high level
else
P3OUT & = ~ BIT1; / / P3.1 output low level
P3OUT | = BIT3; / / SCLK rising edge is generated
data << = 1;
    }
  }
}
```

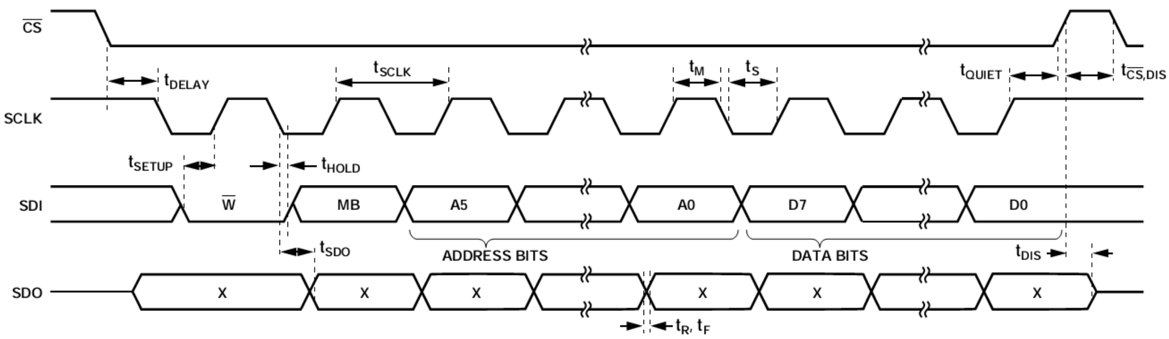

Fig. 6. Four-wire timing of SPI writing.

It should be noted that ADXL345 also returns data when writing on the ADXL345 is done, but this returned data is useless and must be ignored. Reading ADXL345 data subfunction is similar to this. ADXL345 output is in 16-bit data format. Data reconstruction is still needed after acceleration data are obtained from the data register [6]. Details may be found in the ADXL345 data sheet.

Inactivity interrupted set when acceleration value was below a certain threshold (THRESH_INACT), and this lasted for more than a certain time (TIME_INACT) in order to reduce power consumption. The interrupt request was put forward through the MSP430F149 P1.2/TA1 pin, and MSP430F149 writing instruction enabled ADXL345 to be in a dormant state.

6. Experimental Results

Digital inclinometer is achieved using MSP430F149 and ADXL345. Table 1 shows the actual measurement results. It is necessary to measure the zero point offset of each axis before measurement, and an ADXL345 calibration is made. The seriously polluted data are discarded in the measurement results through the software filter [7]. As can be seen from Table 1, the error can be controlled at ±0.3°. Using 2-axis output component ratio of gravitational acceleration in the formula for calculating angle can avoid error caused by the initial position offset of single-axis accelerometer. The measurement angle resolution of the inclinometer may be up to 0.015°.

Table 1. Result of dip angle measurement.

Nominal Angle / °	$\gamma = -\arctan(G_x / G_z)$		$\theta = \arctan(G_y / G_z)$	
	Measured value of pitch angle / °	Error / °	Measured value of roll angle / °	error / °
80	79.782	-0.218	80.217	+0.217
60	60.245	+0.245	59.784	-0.216
50	49.786	-0.214	50.296	+0.296
40	39.815	-0.185	39.718	-0.282
30	30.264	+0.264	29.728	-0.272
15	14.701	-0.299	15.203	+0.203
0	0.215	+0.215	0.245	+0.245

It is found that accelerometer sensitivity is lowest when the angle is close to 0 degree or 90 degrees in actual measurement process. Moreover, the precision of measurement results is lowest. These are caused by a defect of measurement principle itself. There is always a component whose derivative to angle tends to zero in the triaxial components of gravity when angle tends to 0 degree or 90 degrees. It means that sensitivity tends to zero. This is needed to be improved.

ADXL345 triaxial accelerometer with high sensitivity has characteristics such as high integration and low power consumption. Inclination measurement system, composed by ADXL345 triaxial accelerometer and low power MSP430 microcontroller, can not only accurately detect inclination changes, but also greatly reduce overall system power consumption. It can be applied to freefall detection, swing and other inclination measurement occasions under gravity reference system.

Acknowledgements

Project supported by Education Department of Zhejiang Province (NO. Y201223915).

References

[1]. D. Pheifer, P. B. William, The electrolytic tilt sensor, *Sensors Magazine*, Vol. 10, Issue 10, 2000, pp. 325-331.

[2]. J. Ruiting, Accelerometer-based inclination measurement, *Electronics Diy*, Vol.11, 2010, pp. 37-39.

[3]. Yang. Honghong, C. Huijuan, Design of an electronic compass based on magnetoresistance sensor and accelerometer, *Microcomputer & Its Applications,* Vol. 30, Issue 15, 2011, pp. 93-95.

[4]. Analog Devices, Inc.3-Axis, ±2g/±4g/±8g/±16g Digital Accelerometer Sensor ADXL345 [DB/OL]. http://www.analog.com, 2009.

[5]. MSP430xlxx Family User's Guide [DB/OL], *Texas Instruments Incorporated*, 2002.

[6]. N. Jia, Fall Detection Application by Using 3-Axis Accelerometer ADXL345 [DB/OL], *Analog Devices*, 2009.

[7]. E. Candes, J. Romberg, T. Tao, Stable signal recovery from incomplete and inaccurate measurements, *Communication Pure and Applications*, Vol. 59, Issue 8, 2006, pp. 1207-1223.